ACKNOWLEDGMENT

The author wishes to thank Y. Sawayama for many helpful discussions and suggestions, M. Morita for his assistance in noise measurements, I. Kuru and K. Hirai for supplying Gunn diodes and oscillators, and S. Okano and M. Kashiwagi for supplying Si and GaAs avalanche diodes.

REFERENCES

[1] J. Josenhans, "Noise spectra of Read diode and Gunn oscillators," *Proc. IEEE* (Lett.), vol. 54, pp. 1478–1479, Oct. 1966.
[2] J. G. Ondria and J. C. Collinet, "Investigation of noise reduction techniques of solid-state type microwave sources," in *1968 Int. Solid-State Circuits Conf., Dig. Tech. Papers*, pp. 82–83.
[3] E. F. Scherer, "Investigations of the noise spectra of avalanche oscillators," *IEEE Trans. Microwave Theory Tech.* (*Special Issue on Noise*), vol. MTT-16, pp. 781–788, Sept. 1968.
[4] J. R. Ashley and F. M. Palka, "Noise properties and stabilization of Gunn and avalanche diode oscillators and amplifiers," in *1970 G-MTT Int. Microwave Symp. Dig.*, pp. 161–164.
[5] ——, "Reduction of FM noise in microwave diode oscillators by cavity and injection stabilization," in *1971 G-MTT Int. Microwave Symp. Dig.*, pp. 94–95.
[6] W. A. Edson, "Noise in oscillators," *Proc. IRE*, vol. 48, pp. 1454–1466, Aug. 1960.
[7] J. A. Mullen, "Background noise in nonlinear oscillators," *Proc. IRE*, vol. 48, pp. 1467–1473, Aug. 1960.
[8] K. Kurokawa, "Noise in synchronized oscillators," *IEEE Trans. Microwave Theory Tech.*, vol. MTT-16, pp. 234–240, Apr. 1968.
[9] ——, "Some basic characteristics of broadband negative resistance oscillator circuits," *Bell Syst. Tech. J.*, vol. 48, pp. 1937–1955, July–Aug. 1969.
[10] Y. Okabe and S. Okamura, "Analysis of stability and noise of oscillators in free-running, synchronized-running and parallel-running," *J. Inst. Electron. Commun. Eng. Jap.*, vol. 12, pp. 755–762, Dec. 1969.
[11] W. B. Davenport and W. L. Root, *Randon Signals and Noise*. New York: McGraw-Hill, 1958, ch. 6.
[12] L. S. Cutler and C. L. Searle, "Some aspects of the theory and measurement of frequency fluctuations in frequency standards," *Proc. IEEE* (*Special Issue on Frequency Stability*), vol. 54, pp. 136–154, Feb. 1966.
[13] M. E. Hines, "Potential applications and the noise problem in the Read avalanche diode," in *1966 Int. Solid-State Circuits Conf., Dig. Tech. Papers*, pp. 82–83.
[14] M. Ohtomo and Y. Sawayama, "Noise measurement of microwave solid-state oscillators," in *1971 Nat. Conf. Rec. Inst. Electron. Commun. Eng. Jap.*, no. 568.
[15] J. R. Ashley, C. B. Searles, and F. M. Palka, "The measurement of oscillator noise at microwave frequencies," *IEEE Trans. Microwave Theory Tech.* (*Special Issue on Noise*), vol. MTT-16, pp. 753–760, Sept. 1968.
[16] J. G. Ondria, "A microwave system for measurements of AM and FM noise spectra," *IEEE Trans. Microwave Theory Tech.* (*Special Issue on Noise*), vol. MTT-16, pp. 767–781, Sept. 1968.
[17] A. A. Sweet and L. A. MacKenzie, "The FM noise of a CW Gunn oscillator," *Proc. IEEE* (*Special Issue on Detection Theory and Its Applications*) (Lett.), vol. 58, pp. 822–823, May 1970.
[18] E. F. Scherer, "Circuit techniques for the noise reduction and frequency stabilization of avalanche diode oscillators," in *1968 G-MTT Int. Microwave Symp. Dig.*, pp. 63–71.
[19] M. Kashiwagi, S. Okano, T. Utagawa, and M. Takabayashi, "GaAs IMPATT diode," in *1970 Joint Conv. Rec. Four Inst. Electron. Eng. Jap.*, no. 1743.
M. Kashiwagi, T. Utagawa, S. Okano, and M. Ohtomo, "X-band GaAs IMPATT diode," *Inst. Electron. Commun. Eng. Jap.*, Nov. 1970, ED 70-31.
[20] D. L. Scharfetter and H. K. Gummel, "Large-signal analysis of a silicon Read diode oscillator," *IEEE Trans. Electron Devices*, vol. ED-16, pp. 64–77, Jan. 1969.
[21] M. Ohtomo, "Reflection-type IMPATT diode power amplifier for 11-GHz band," *Inst. Electron. Commun. Eng. Jap.*, July 1970, ED 70-14.
[22] C. G. Montgomery, R. H. Dicke, and E. M. Purcell, *Principles of Microwave Circuits*, M.I.T. Rad. Lab. Series 8. New York: McGraw-Hill, 1948, ch. 4, 5, and 7.

First-Order Nonlinear Theory in Hexagonal Ferrites with Planar Anisotropy under Perpendicular Pumping

JOSEPH HELSZAJN, MEMBER, IEEE, AND JOHN MCSTAY

Abstract—**The first-order spinwave instability under perpendicular pumping at large signal power in an hexagonal ferrite ellipsoid with planar anisotropy biased in the easy plane is studied. The nonlinear coupling coefficient is obtained in terms of the physical variables of the unstable spinwaves and the uniform mode magnetization such as the orientation and ellipticity of the unstable spinwaves, the coordinates of the spinwave propagation vector *k*, and the uniform mode ellipticity. Results obtained using a computer in the case of a sphere are included. Also included are experimental results on the coincidence region with the dc field in the easy plane and with the dc field out of the easy plane. This latter arrangement leads to a new tunable coincidence limiter.**

Manuscript received February 5, 1970; revised August 19, 1970. This work was supported by the Ministry of Technology, England.
J. Helszajn is a consultant, 3 Abercromby Place, Edinburgh 3, Scotland.
J. McStay is with the Department of Electronic Engineering, the University of Leeds, Leeds, England.

I. INTRODUCTION

THE first- and second-order nonlinear behavior in isotropic ferrites under perpendicular pumping at large signal power due to spinwave instabilities are well known [1]–[5]. The first-order nonlinear process is usually the more important one and is the only one considered in this paper. This instability gives rise to an additional subsidiary resonance peak below the magnetic field required for the main resonance. Under some circumstances it is also possible for the subsidiary resonance and the main resonance to occur simultaneously. The critical RF magnetic field threshold is then particularly low (coincidence limiting). The onset of spinwave instability at the subsidiary resonance peak arises from parametric coupling between the uniform mode and spinwaves. The important spinwaves are those which are synchronous with half the excitation frequency.

The theory of spinwave instability in anisotropic ferrites with planar anisotropy biased in the easy plane has also been described, but the instability threshold has not been minimized [6], [7]. These planar ferrites possess an easy plane of magnetization perpendicular to the C axis of the crystal [8]. This effective planar anisotropy field alters the isotropic linear parts of both the uniform mode of magnetization and the spinwave modes, and also the nonlinear coupling between the two. In addition, the propagation vector k of the unstable spinwave for this form of instability has now an azimuthal dependence ϕ_k in addition to the usual polar dependence θ_k.

The usual theory combines the nonlinear coupled component equations of the transverse part of the equation of motion into a single equation with the help of complex variables. Since the normal variables are in general elliptical a Holstein–Primakoff transformation is then required to reduce the equation to a normal form in terms of circular variables [9]. The disadvantage of this method is that it moves the final result through two transformations from the physical problem.

The purpose of this paper is to develop the theory of spinwave instability in planar ferrites in terms of the physical variables of the spinwave and uniform normal modes. The final transformation to circular variables is thereby simplified and the important physical parameters, i.e., the orientation and ellipticity of the unstable spinwaves, the coordinates of the spinwave propagation vector k, and the uniform mode ellipticity, appear explicitly in the final transformation.

The instability threshold has been minimized using a computer for the case of a sphere with the effective anisotropy field as a variable and butterfly curves have been obtained. As the dc field is increased from zero, the butterfly curve consists of two branches which correspond to the two regions obtained from the dispersion relation in which the unstable spinwaves have either $k \neq 0$ or $k = 0$. The spinwaves with $k \neq 0$ propagate in the easy plane at about 45° with respect to the dc field. The spinwaves with $k = 0$ propagate in the easy plane with an angle less than 45° with respect to the dc field. The dispersion relation ceases to yield a real value of k when the angle between the dc field and the unstable spinwaves approaches zero.

The primary effect of increasing the effective anisotropy field is to lower the RF threshold for spinwave instability, and to shift the dc field corresponding to the minimum of the butterfly curve from below that required for ferrimagnetic resonance to the coincidence

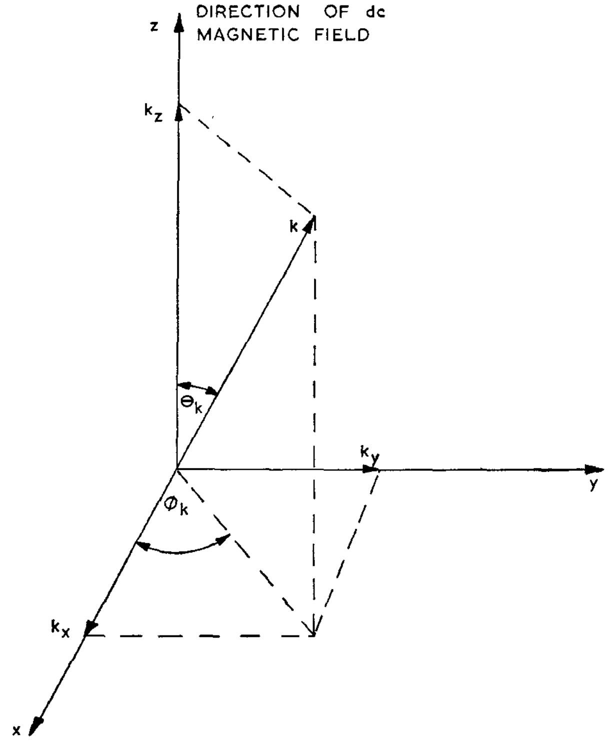

Fig. 1. Rectangular coordinate system.

region and finally to a dc field larger than that required for the main resonance.

II. Nonlinear Equation of Motion

The equation of motion of the magnetization is

$$\dot{\overline{M}} = -\gamma(\overline{M} \times \overline{H}) + \text{dissipation term} \tag{1}$$

where $\overline{M}$ is the total magnetization, $\overline{H}$ is the total magnetic field, and γ is the gyromagnetic ratio. The dissipation term will be introduced phenomenologically later on by adding an imaginary part to the frequency.

Following Suhl the deviation of the magnetization due to the exchange field is expanded in a Fourier series of spinwaves

$$\overline{M} = \overline{M}_0 + \bar{m}_0 e^{i\omega t} + \sum_{k \neq 0} \bar{m}_k e^{i(\bar{k}\cdot\bar{r} + \omega_k t)} \tag{2}$$

where $\overline{M}_0$ is the dc magnetization, $\bar{m}_0$ is the RF magnetization, $\bar{m}_k$ is the spinwave magnetization, and $\bar{r}$ is a radius vector. Hereafter, the time and spatial dependence of the magnetization will be taken for granted.

The total magnetic field in the case of a spheroid in terms of the rectangular coordinate system in Fig. 1 is given by

$$\overline{H} = \overline{H}_0 + \bar{h} + \overline{H}_{\text{dem}} + \bar{h}_{\text{dem}} + \overline{H}_{\text{ex}} + \overline{H}_{\text{dip}} + \overline{H}_a. \tag{3}$$

The first four terms are the usual dc field, RF field, and demagnetizing fields. The effective exchange field $\overline{H}_{\text{ex}}$ is derived from the exchange energy, which is an energy of electrostatic origin and has no classical counterpart. The dipolar field $\overline{H}_{\text{dip}}$ is a demagnetizing field which is derived from Maxwell's equation boundary conditions being neglected. The last field is the effective anisotropy field $\overline{H}_a$ due to the planar anisotropy of the ferrite material. For a hexagonal single crystal ferrite with the easy plane in the y–z plane and the hard axis along the x coordinate, the effective anisotropy field consists of two terms; one proportional to the x component of the uniform mode magnetization, and the other proportional to the x component of the spinwave magnetization. This last effective field modifies the linear parts of both the uniform mode and the spinwave modes, and also the nonlinear coupling between the two. It is this effective field that we shall study in this paper.

In component form the fields in (3) are

$$\overline{H}_0 = \begin{bmatrix} 0 \\ 0 \\ H_0 \end{bmatrix} \tag{4}$$

$$\bar{h} = \begin{bmatrix} h_x \\ h_y \\ 0 \end{bmatrix} \tag{5}$$

$$\overline{H}_{\text{dem}} = -\begin{bmatrix} 0 \\ 0 \\ N_z \dfrac{M_0}{\mu_0} \end{bmatrix} \tag{6}$$

$$\bar{h}_{\text{dem}} = -\begin{bmatrix} N_t \dfrac{M_0}{\mu_0} \\ N_t \dfrac{M_0}{\mu_0} \\ 0 \end{bmatrix} \tag{7}$$

$$\overline{H}_{\text{ex}} = -\frac{H_{\text{ex}}a^2}{M_0}\begin{bmatrix} \sum_{k\neq 0} k^2 m_{kx} \\ \sum_{k\neq 0} k^2 m_{ky} \\ \sum_{k\neq 0} k^2 m_{kz} \end{bmatrix} \tag{8}$$

$$\overline{H}_{\text{dip}} = -\begin{bmatrix} \sum_{k\neq 0} k_x k^{-2}\left(k_x \dfrac{m_{kx}}{\mu_0} + k_y \dfrac{m_{ky}}{\mu_0} + k_z \dfrac{m_{kz}}{\mu_0}\right) \\ \sum_{k\neq 0} k_y k^{-2}\left(k_x \dfrac{m_{kx}}{\mu_0} + k_y \dfrac{m_{ky}}{\mu_0} + k_z \dfrac{m_{kz}}{\mu_0}\right) \\ \sum_{k\neq 0} k_z k^{-2}\left(k_x \dfrac{m_{kx}}{\mu_0} + k_y \dfrac{m_{ky}}{\mu_0} + k_z \dfrac{m_{kz}}{\mu_0}\right) \end{bmatrix} \tag{9}$$

$$\overline{H}_a = -\begin{bmatrix} \dfrac{H_a}{M_0}(m_{0x} + m_{kx}) \\ 0 \\ 0 \end{bmatrix} \tag{10}$$

where we have assumed that $M_0 \gg m_{0z}$.

Here N_t and N_z are transverse and longitudinal dc demagnetizing factors, a is the lattice constant, and k_x, k_y, and k_z are wavenumbers along the axis of the coordinate system shown in Fig. 1.

If the spinwave amplitudes are all assumed to be much smaller than the amplitude of the uniform mode, the longitudinal component m_{kz} can be given in terms of the transverse components because the magnetization in any small volume is conserved.

$$M^2 = \left(m_{0x} + \sum_{k\neq 0} m_{kx}\right)^2 + \left(m_{0y} + \sum_{k\neq 0} m_{ky}\right)^2 + \left(M_0 + \sum_{k\neq 0} m_{kz}\right)^2. \tag{11}$$

Equating the spatially varying terms we have

$$\sum_{k\neq 0} m_{kz} = -\frac{1}{M_0}\left(m_{0x}\sum_{k\neq 0} m_{kx} + m_{0y}\sum_{k\neq 0} m_{ky}\right). \tag{12}$$

As long as this approximation is valid, it is sufficient to consider a single typical spinwave term and we will hereafter omit the summation sign for clarity and simplicity. If we expand the equation of motion, omit higher order powers of the spinwave amplitude, and write m_{kz} in terms of m_{kx} and m_{ky} with the help of (12) we obtain

$$\begin{aligned}(\dot{m}_{0x} + \dot{m}_{kx}) = &- m_{0y}(\omega_0 - N_z\omega_m + N_t\omega_m) + \mu_0\omega_m h_y \\ &- m_{ky}(\omega_0 - N_z\omega_m + k_y{}^2k^{-2}\omega_m + \omega_{\text{ex}}) \\ &- m_{kx}k_xk_yk^{-2}\omega_m + m_{kx}(k_xk_zk^{-2}\omega_m)\frac{m_{0y}}{M_0} \\ &+ m_{ky}(2k_yk_zk^{-2}\omega_m)\frac{m_{0y}}{M_0} \\ &+ m_{kx}(k_yk_zk^{-2}\omega_m)\frac{m_{0x}}{M_0}\end{aligned} \tag{13}$$

$$\begin{aligned}(\dot{m}_{0y} + \dot{m}_{ky}) = &\ m_{0x}(\omega_0 - N_z\omega_m + N_t\omega_m + \omega_a) - \mu_0\omega_m h_x \\ &+ m_{kx}(\omega_0 - N_z\omega_m + k_x{}^2k^{-2}\omega_m + \omega_{\text{ex}} + \omega_a) \\ &+ m_{ky}k_xk_yk^{-2}\omega_m - m_{ky}(k_yk_zk^{-2}\omega_m)\frac{m_{0x}}{M_0} \\ &- m_{kx}(2k_xk_zk^{-2}\omega_m)\frac{m_{0x}}{M_0} \\ &- m_{ky}(k_xk_zk^{-2}\omega_m)\frac{m_{0y}}{M_0}\end{aligned} \tag{14}$$

where

$$\omega_m = \frac{\gamma M_0}{\mu_0}, \qquad \omega_0 = \gamma H_0, \qquad \omega_{\text{ex}} = \gamma H_{\text{ex}}a^2k^2,$$

and

$$\omega_a = \gamma H_a.$$

Equations (13) and (14) are the nonlinear transverse component equations of the magnetization. These equations can be divided into three parts: terms involving the uniform mode, terms involving the linear part of the spinwave mode, and nonlinear terms proportional to the first-order of the uniform mode amplitude.

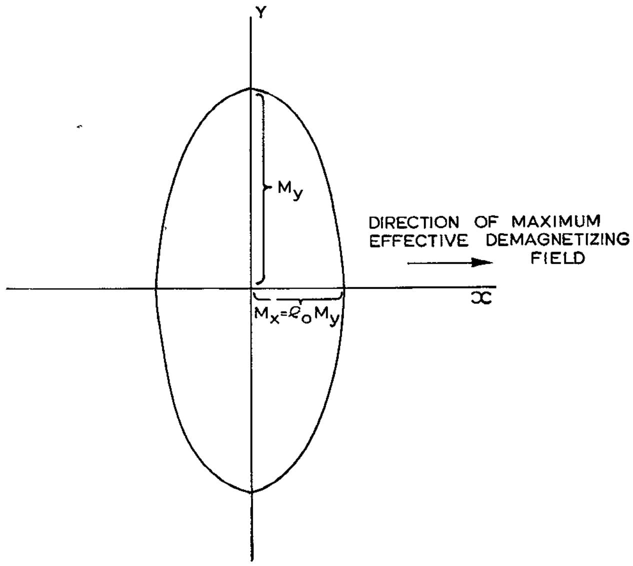

Fig. 2. Uniform mode ellipse in transverse plane at resonance.

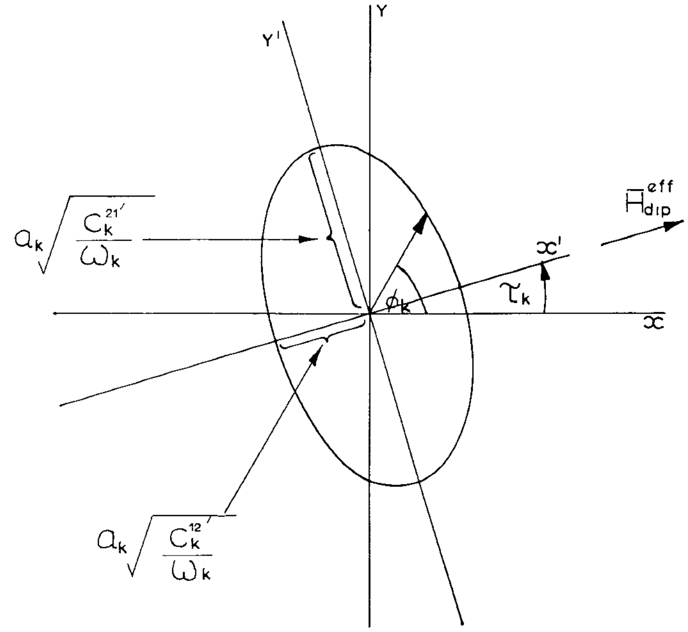

Fig. 3. Spinwave ellipse in transverse plane.

III. Uniform Mode

The uniform part of the nonlinear equation of magnetization can be obtained from (13) and (14) by equating the nonspatially varying terms. It is assumed that the RF field is in the easy plane. We therefore have $h_x = 0$, $h_y = h_0 \sin \omega t$. Hence

$$m_{0x} = \left(\frac{\mu_0 \omega_m \omega}{-\omega^2 + \omega_r^2}\right) h_0 \cos \omega t \tag{15}$$

$$m_{0y} = \frac{1}{e_0}\left(\frac{\mu_0 \omega_m \omega_r}{-\omega^2 + \omega_r^2}\right) h_0 \sin \omega t \tag{16}$$

where

$$\omega_r^2 = \omega_x \omega_y \tag{17}$$

$$e_0^2 = \frac{\omega_y}{\omega_x} \tag{18}$$

and

$$\omega_x = (\omega_0 - N_z \omega_m + N_t \omega_m + \omega_a) \tag{19}$$

$$\omega_y = (\omega_0 - N_z \omega_m + N_t \omega_m). \tag{20}$$

In the preceding equations, ω_r is the well-known Kittel resonance frequency and e_0 is the uniform mode ellipticity at the main resonance. The uniform mode ellipse is shown in Fig. 2. The uniform mode ellipticity is given in [10] as a function of ω_0/ω for parametric values ω_a/ω for the relevant range of this work.

IV. Linear Part of Spinwave Equations

The linear part of the spinwave equation is from (13) and (14) given by

$$\dot{m}_{kx} = -m_{ky}(\omega_0 - N_z\omega_m + \omega_m k_y^2 k^{-2} + \omega_{ex}) - m_{kx}(\omega_m k_x k_y k^{-2}) \tag{21}$$

$$\dot{m}_{ky} = m_{kx}(\omega_0 - N_z\omega_m + \omega_m k_x^2 k^{-2} + \omega_{ex} + \omega_a) + m_{ky}(\omega_m k_x k_y k^{-2}). \tag{22}$$

The preceding equations are the same as those found in the case of parallel pumping [11]. The general solution to these equations is of the form of an ellipse with the major axis tilted through an angle τ_k, as shown in Fig. 3. The minor axis of the ellipse is orientated along the direction of maximum internal demagnetizing field.

This solution has been shown to be considerably simplified if a coordinate transformation is introduced which aligns the ellipse with a new coordinate system whose axes are rotated by the angle τ_k. The result is

$$m_{kx'} = \left(\frac{C_k^{12'}}{\omega_k}\right)^{1/2} a_k \cos \omega_k t \tag{23}$$

$$m_{ky'} = \left(\frac{C_k^{21'}}{\omega_k}\right)^{1/2} a_k \sin \omega_k t \tag{24}$$

where

$$\omega_k^2 = C_k^{12'} C_k^{21'} \tag{25}$$

and a_k is an amplitude constant. The last equation is the well-known dispersion relation.

The ratio of the minor axis to the major axis of the ellipse is given by

$$e_k = \left(\frac{C_k^{12'}}{C_k^{21'}}\right)^{1/2}. \tag{26}$$

$C_k^{12'}$ and $C_k^{21'}$ are given in terms of the original variables in [11].

V. First-Order Spinwave Instability

The first-order nonlinear spinwave instability is usually the most important one because the amplitude of the uniform mode is usually quite small even in the nonlinear region. Introducing the coordinate transformation developed in [11] into the first-order nonlinear equations gives

$$\dot{m}_{kx'} = -C_k^{12'}m_{ky'} + m_{kx'}\{m_{0x}[-\sin(2\tau_k-\phi_k)] + m_{0y}[\cos(2\tau_k-\phi_k)]\}\frac{\gamma}{M_0}\sin\theta_k\cos\theta_k + m_{ky'}\{m_{0x}[\cos\phi_k-\cos(2\tau_k-\phi_k)] + m_{0y}[\sin\phi_k-\sin(2\tau_k-\phi_k)]\}\frac{\gamma}{M_0}\sin\theta_k\cos\theta_k \quad (27)$$

$$\dot{m}_{ky'} = C_k^{21'} - m_{kx'}\{m_{0x}[\cos\phi_k+\cos(2\tau_k-\phi_k)] + m_{0y}[\sin\phi_k+\sin(2\tau_k-\phi_k)]\}\frac{\gamma}{M_0}\sin\theta_k\cos\theta_k - m_{ky'}\{m_{0x}[-\sin(2\tau_k-\phi_k)] + m_{0y}[\cos(2\tau_k-\phi_k)]\}\frac{\gamma}{M_0}\sin\theta_k\cos\theta_k. \quad (28)$$

In this paper the various nonlinear thresholds are obtained in terms of the components along the minor axis of the spinwave ellipse.

By introducing complex variables the relation between the transverse components of magnetization of the uniform mode is given from (15) and (16)

$$m_{0x} = (m_0 + m_0^*) \quad (29)$$

$$m_{0y} = \left(\frac{\omega_r}{\omega}\right)\left(\frac{m_0 - m_0^*}{ie_0}\right) = \frac{m_0 - m_0^*}{ie} \quad (30)$$

where

$$m_0 = \left(\frac{\mu_0\omega_m\omega}{-\omega^2+\omega_r^2}\right)\frac{h_0e^{i\omega t}}{2} \quad (31)$$

m_0^* is the complex conjugate equation, and $e = (\omega/\omega_r)e_0$.

The relation between the transverse components of magnetization of the linear part of the spinwave mode is given from (23) and (24).

Using the preceding identities the nonlinear coupled equations can be reduced to a single equation given by

$$\dot{m}_k = i\omega_k m_k + im_k^*|f_k|m_0 \quad (32)$$

where f_k the coupling coefficient is given by

$$|f_k| = \left\{\left[\left(1+\frac{e^{-1}e_k^{-1}}{2}+\frac{e^{-1}e_k}{2}\right)\sin(2\tau_k-\phi_k) + \left(\frac{e^{-1}e_k}{2}-\frac{e^{-1}e_k^{-1}}{2}\right)\sin\phi_k\right]^2 + \left[\left(e^{-1}+\frac{e_k^{-1}}{2}+\frac{e_k}{2}\right)\cos(2\tau_k-\phi_k) + \left(\frac{e_k}{2}-\frac{e_k^{-1}}{2}\right)\cos\phi_k\right]^2\right\}^{1/2}\frac{\gamma}{\mu_0}\sin\theta_k\cos\theta_k. \quad (33)$$

Nonsynchronous terms have been omitted in (33). Hence the important spinwaves are those that are synchronous with half the frequency of the RF excitation.

An approximate solution to (32) is of the form $m_k\exp(i(\omega/2+iK)t)$, where K is an adjustable parameter to be determined. Substituting this approximate solution into (32) we obtain the standard result for the instability threshold

$$|m_0|_{\text{crit}} > \frac{\left[\left(\omega_k-\frac{\omega}{2}\right)^2+\left(\frac{\gamma\Delta H_k}{2}\right)^2\right]^{1/2}}{|f_k|} \quad (34)$$

where we have taken the damping of the spinwave into account by adding a positive imaginary part $\gamma\Delta H_k/2$ to ω_k, where ΔH_k is the spinwave linewidth. We now write $|m_0|$ in terms of $|h_0|$ with the help of (31); hence

$$|h_0|_{\text{crit}} = \frac{2\left[\left(\omega_k-\frac{\omega}{2}\right)^2+\left(\frac{\gamma\Delta H_k}{2}\right)^2\right]^{1/2}\left[(\omega_r^2-\omega^2)^2+4\omega_r^2\left(\frac{\gamma\Delta H}{2}\right)^2\right]^{1/2}}{\mu_0\omega_m|f_k|}. \quad (35)$$

In the last equation the damping to the uniform mode is accounted for by introducing a positive imaginary part $\gamma\Delta H/2$ to ω_r in (31), where ΔH is the uniform mode linewidth. From the numerator of (35) we see that $2\omega_k=\omega$, or $\omega_r=\omega$, or both conditions produce a sharp reduction in $|h_0|_{\text{crit}}$.

VI. Minimization Procedure

In order to find the lowest threshold we have to minimize the right-hand side of (35) as the applied dc field is varied subject to the side condition $\omega_k=\omega/2$.

From the dispersion relation at the subsidiary resonance we have

$$\omega_{\text{ex}} = \tfrac{1}{2}[(\omega_m\sin^2\theta_k+\omega_a)^2+\omega^2-4\omega_a\omega_m\sin^2\theta_k\sin^2\phi_k]^{1/2} - \tfrac{1}{2}(\omega_m\sin^2\theta_k+\omega_a)-(\omega_0+N_z\omega_m). \quad (36)$$

As the applied field is increased from zero the dispersion relation consists of two regions where $k\neq 0$ and $k=0$.

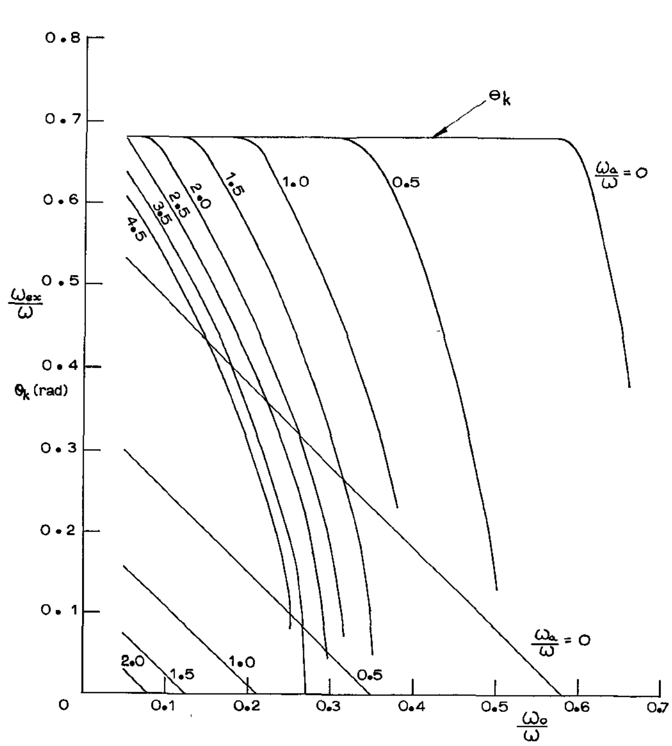

Fig. 4. Coordinates of unstable spinwave (unstable spinwave is always in easy plane, $\phi_k = 90°$).

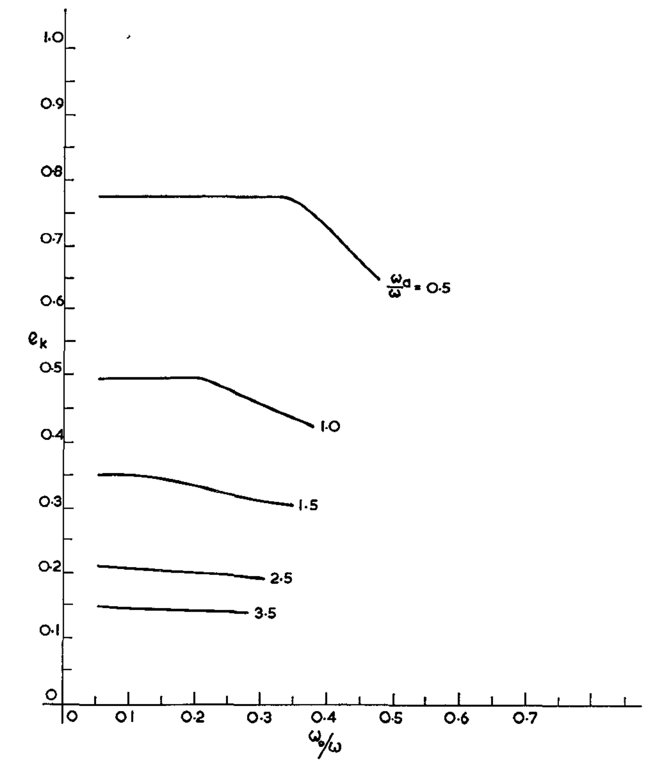

Fig. 5. Unstable spinwave ellipticity as a function of dc field ω_0/ω with $\omega_m/\omega = 0.60$.

Equation (35) has been minimized using a computer in the case of a sphere as a function of the dc field ω_0/ω for parametric values of ω_a/ω with $\omega_m/\omega = 0.6$ subject to the frequency condition given by (36). The computer printout included θ_k, ϕ_k, ω_{ex}, e_k, ω_r, ω_0, e_0, and f_k. In the region where $k \neq 0$ the frequency relation involves k, θ_k, and ϕ_k.

The coordinates of the unstable spinwaves in the two regions where $k \neq 0$ and $k = 0$ are shown in Fig. 4. In the region where $k \neq 0$, the unstable spinwave propagates in the easy plane ($\phi_k = 90°$) with θ_k approximately given by $\theta_k \approx 45°$.

In the region where $k = 0$, the allowed values of θ_k and ϕ_k are uniquely related by (36) with $\omega_{ex} = 0$ once the dc field is stated. In this region the minimum of the butterfly curve occurred with $\phi_k = 90°$ also and with θ_k determined from the frequency relation by

$$\sin^2 \theta_k = \frac{\frac{\omega^2}{4} - (\omega_0 - N_z\omega_m)(\omega_0 - N_z\omega_m + \omega_a)}{\omega_m(\omega_0 - N_z\omega_m)}. \tag{37}$$

The dispersion relation ceases to yield a real value for k with $\theta_k = 0$ at a magnetic field given by

$$\omega_0 = \frac{-\omega_a + \sqrt{\omega_a^2 + \omega^2}}{2} + N_z\omega_m. \tag{38}$$

This last equation provides a convenient rule for the existence of the subsidiary resonance.

The unstable spinwave ellipticity is shown in Fig. 5. Fig. 6 shows the RF threshold as a function of the resonant field ω_r/ω for parametric values of ω_a/ω with $\omega_m/\omega = 0.6$. Fig. 7 shows the same quantities as a function of the dc field ω_0/ω. From these two graphs we see that one effect of the anisotropy field is to lower the RF threshold field. Another effect is to shift the minimum of the butterfly curve from a dc field below that required for the main resonance through the coincidence region to a dc field larger than that required for the main resonance. In the coincidence region the butterfly curve is seen to go to zero. This occurs because we have omitted the uniform mode damping $\gamma\Delta H/2$ in our calculations.

In the easy plane f_k is given with $\tau_k = 0°$ for $\omega_a/\omega > \omega_m \sin^2 \theta_k/\omega$, and with $\tau_k = 90°$ for $\omega_a/\omega < \omega_m \sin^2 \theta_k/\omega$. For $\omega_a/\omega = \omega_m \sin^2 \theta_k/\omega$ the spinwave ellipticity is unity and f_k is independent of τ_k.

For $\omega_a/\omega > \omega_m \sin^2 \theta_k/\omega$, (33) becomes

$$f_k = (1 + e^{-1}e_k^{-1}) \frac{\omega_m}{M_0} \sin \theta_k \cos \theta_k. \tag{39}$$

VII. Coincidence of Subsidiary and Main Resonances

As we can see from Fig. 7, it is possible for certain configurations to satisfy the condition $\omega_k = \omega/2$ simultaneously with $\omega_r = \omega$. The critical field for the onset of the spinwave instability is then particularly low. Such limiting has been reported in single crystal YIG

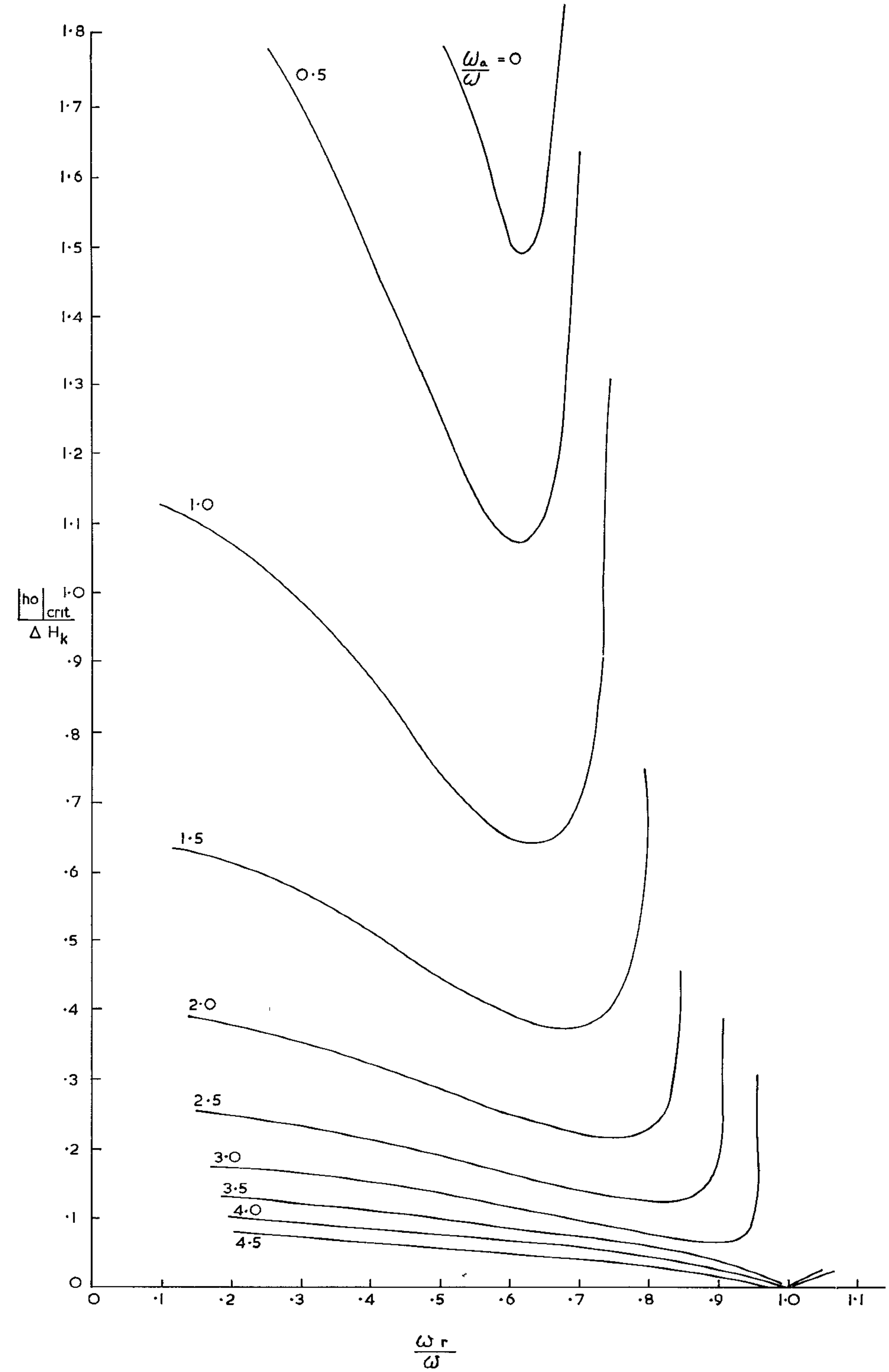

Fig. 6. RF threshold as a function of the resonant field ω_r/ω for parametric values of ω_a/ω with $\omega_m/\omega = 0.6$.

[12], [13]. The lowest threshold now occurs at the main resonance and causes a reduction of the susceptibility at resonance. This is clearly shown in Fig. 7. For the coincidence condition to hold we must satisfy the frequency condition given by (36) with $\theta_k = 0$. This condition is only satisfied at low frequencies. Since the sample must be magnetically saturated the frequency range of application is [6], [15]

$$[\omega_m N_t(\omega_m N_t + \omega_a)]^{1/2} < \omega < \frac{2}{3} N_t\omega_m \left\{5 + 4\left[1 + \left(\frac{3\omega_a}{4N_t\omega_m}\right)^2\right]^{1/2}\right\}^{1/2}. \quad (40)$$

Equation (40) shows that the effect of the anisotropy field is to reduce the coincidence region. Fig. 8 shows the coincidence region obtained for a sample of $Mn\text{–}Zn_2Y$ single crystal ferrite biased in the easy plane. The ma-

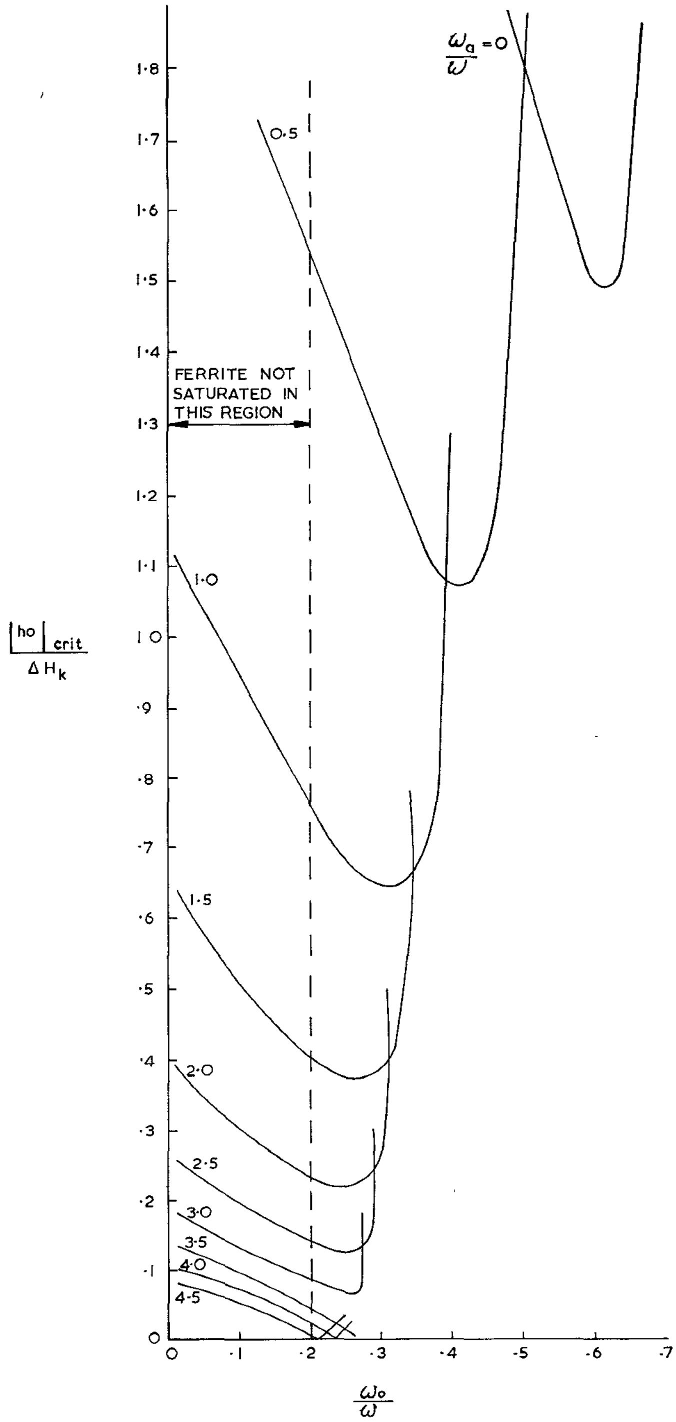

Fig. 7. RF threshold as a function of the dc field ω_0/ω for parametric values ω_a/ω with $\omega_m/\omega = 0.6$.

terial used was an Mn substituted Zn_2Y single crystal ferrite sphere with $\Delta H = 716$ Am^{-1}, $M_0 = 0.24$ Wm^{-2}, $H_a = 783.8$ kAm^{-1}, and $\gamma = 2.060 \times 10^5$ rad s^{-1}/Am^{-1}.

For a linearly polarized wave in the easy plane, the RF threshold is

$$|h_0|_{crit} = \frac{2\Delta H \Delta H_k}{(1 + e_0^{-1} e_k^{-1}) M_0/\mu_0}. \tag{41}$$

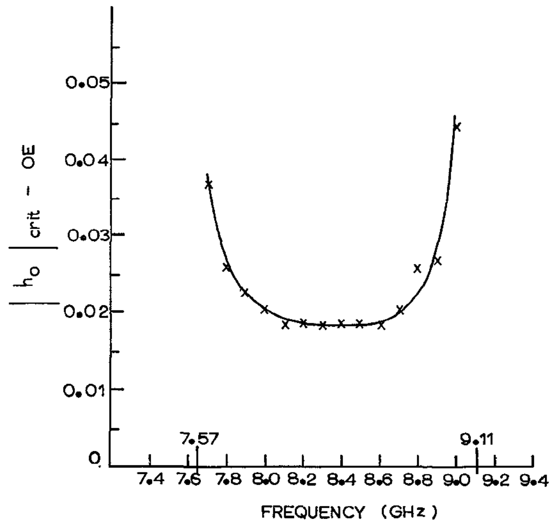

Fig. 8. Coincidence threshold in an Mn–Zn_2Y single crystal ferrite biased in the easy plane.

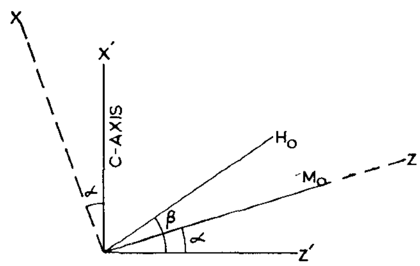

Fig. 9. Coordinates for bias out of easy plane.

Equation (41) can be used to obtain the spinwave linewidth.

An approximate equation for the critical field in the coincidence region has also been given in [6]. However, it is not possible to make a direct comparison with it because the geometric factor A given in this reference does not coincide with the magnetic quantities used here.

An absolute value for ΔH_k has not been obtained because the authors did not obtain ΔH in the coincidence region. It is well known that the uniform mode linewidth is a function of the direct magnetic field [16], [17], [18].

VIII. Coincidence of Subsidiary and Main Resonances with the DC Field Out of the Easy Plane

It is also possible to obtain coincidence limiting in planar single crystal ferrite spheres biased out of the easy plane. This leads to a new tunable coincidence limiter. In the experimental arrangement considered here the dc field H_0 makes an angle β with the easy plane of the crystal which is assumed to be in the y–z' plane and the c axis of the crystal lies along the x' axis of the coordinate system, shown in Fig. 9. The prime coordinate introduced here is not to be mistaken with the one

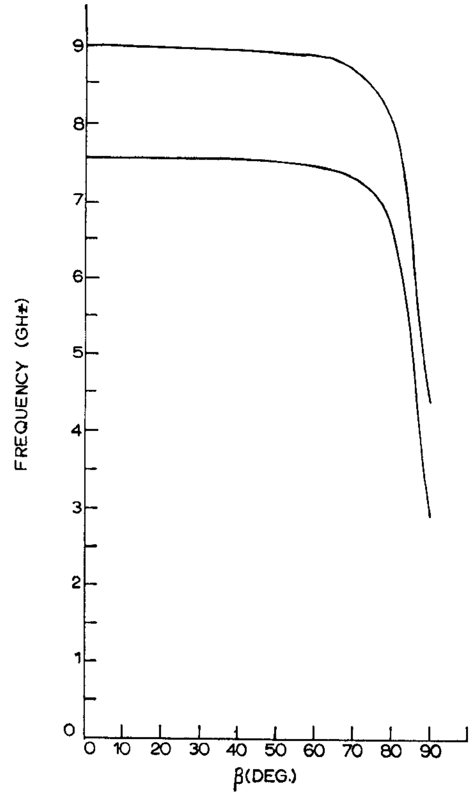

Fig. 10. Coincidence region for Mn–Zn_2Y ferrite sphere biased out of easy plane.

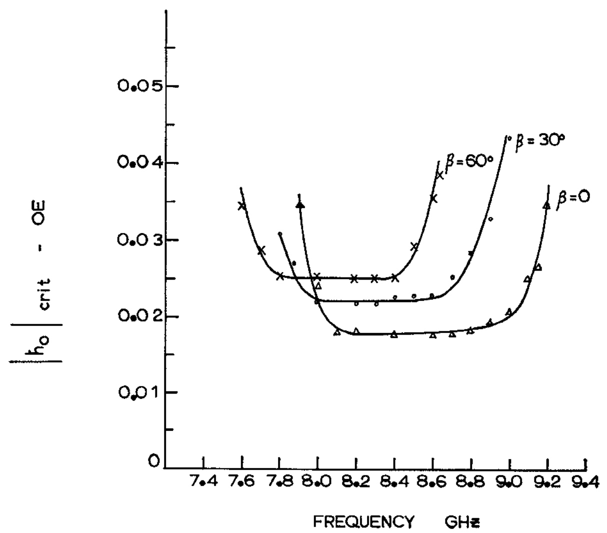

Fig. 11. Coincidence threshold in Mn–Zn_2Y ferrite sphere biased out of easy plane.

introduced in connection with Fig. 3. With this arrangement the magnetization M_0 is no longer in the easy plane but makes an angle α to it, where in the case of a sphere α is determined by [14]

$$2H_0 \sin(\beta - \alpha) = H_a \sin 2\alpha. \tag{42}$$

In the perpendicular pump arrangement the RF field is perpendicular to the magnetization M_0. In what follows the resultant direction of M_0 is therefore taken along the unprimed z axis in Fig. 9. This means that the unprimed transverse plane makes an angle α to the c axis of the crystal. In the plane perpendicular to the magnetization the linear parts of the spinwave and uniform modes have the same form as when the dc magnetization is in the easy plane provided new effective dc and anisotropy fields are defined [10], [11].

$$H_0' = H_0 \cos(\beta - \alpha) - H_a \sin^2 \alpha \tag{43}$$

$$H_a' = H_a \cos^2 \alpha. \tag{44}$$

Tilting the dc field out of the easy plane therefore alters the spinwave dispersion relation and Kittel's resonance frequency.

In calculating the coincidence region it has been assumed that the spinwave that first becomes unstable in the unprimed transverse plane has the same coordinates as in the case when the dc field is in the easy plane. The coincidence region is therefore given by (40) with ω_a and ω_0 replaced by ω_a' and ω_0'.

For the Mn–Zn_2Y single crystal ferrites studied in this paper the coincidence region extends from 7550 to 9000 MHz when the dc field is in the easy plane and from 2900 to 4350 MHz when the dc field is perpendicular to the easy plane. This is shown in Fig. 10. When the dc field is perpendicular to the easy plane it is of the order of the effective anisotropy field.

Fig. 11 shows the experimental coincidence region obtained with an Mn–Zn_2Y single crystal ferrite sphere for three different values of β. In the arrangement used the RF field was in the easy plane along the y axis of the crystal.

IX. Conclusions

The onset of the nonlinear spinwave instability at large RF power which can occur in hexagonal ferrites with planar anisotropy has been derived. This has been done in a simple way in terms of the physical variables of the uniform and spinwave normal modes. The measured coincidence region is in good agreement with the theoretical results. Coincidence measurements are also given with the dc field out of the easy plane. This leads to a new tunable coincidence limiter.

References

[1] R. W. Damon, "Relaxation effects in ferromagnetic resonance," *Rev. Mod. Phys.*, vol. 25, 1953, pp. 239–245.
[2] H. Suhl, "The nonlinear behavior of ferrites at high microwave signal levels," *Proc. IRE*, vol. 44, Oct. 1956, p. 1270.
[3] E. Schlömann, "Ferromagnetic resonance at high power levels," Raytheon Co., Tech. Rep. R-48, 1959.
[4] J. Kemanis and S. Wong, "Analysis of high power effects in ferromagnetics from the point of view of energy transfer, Pt. 1: First-order instabilities," *J. Appl. Phys.*, vol. 35, 1964, pp. 1465–1470.
[5] J. Helszajn and J. McStay, "Simplified theory of nonlinear phenomena in ferromagnetic materials," *Proc. Inst. Elec. Eng.*, vol. 114, Nov. 1967.
[6] I. Bady and E. Schlömann, "Spinwave excitation in planar ferrites," *J. Appl. Phys.*, vol. 33, 1962, p. 1377.

[7] E. Schlömann, R. J. Joseph, and I. Bady, "Spinwave instability in hexagonal ferrites with a preferential plane," *J. Appl. Phys.*, vol. 34, 1963, pp. 672–681.
[8] I. Bady, "Ferrites with planar anistropy at microwave frequencies," *IRE Trans. Microwave Theory Tech.*, vol. MTT-9, Jan. 1961, pp. 52–62.
[9] T. Holstein and H. Primakoff, "Field dependence of the intrinsic domain magnetization of a ferromagnet," *Phys. Rev.*, vol. 58, 1940, p. 1058.
[10] J. Helszajn and J. McStay, "External susceptibility tensor of magnetized ferrite ellipsoid in terms of uniform-mode ellipticity," *Proc. Inst. Elec. Eng.*, vol. 116, Dec. 1969.
[11] ——, "Parallel pumping in hexagonal ferrites with the dc field off the easy plane," *IEEE Trans. Microwave Theory Tech.*, vol. MTT-18, Sept. 1970, pp. 518–524.
[12] E. G. Spencer, R. C. LeCraw, and C. G. Porter, "Ferromagnetic resonance in yttrium iron garnet at low frequencies," *J. Appl. Phys.*, vol. 29, 1958, p. 429.
[13] F. C. Rossol, "Subsidiary resonance in the coincidence region in yttrium iron garnet," *J. Appl. Phys.*, vol. 31, 1960, p. 2273.
[14] D. C. Stinson and M. A. Green, Jr., "Resonance properties of single-crystal ferrites over X-band frequencies," *IEEE Trans. Magn.*, vol. MAG-1, Dec. 1965, pp. 414–416.
[15] W. E. Courtney, "Spinwave instabilities in ferrimagnetic insulators, Part 1," Dept. of Elec. Eng., Univ. of Leeds, Leeds 2, England, Internatl. Rep., Nov. 1964.
[16] C. R. Buffler, *J. Appl. Phys.*, vol. 30, p. 172s, 1959.
[17] Q. H. F. Vrehen, H. G. Beljers, and J. G. M. de Lau, "Microwave properties of fine-grain Ni and Mg ferrites," presented at the 1969 INTERMAG Conf., Amsterdam, The Netherlands, Paper 28.4; also *IEEE Trans. Magn.*, vol. MAG-5, pp. 617–621, Sept. 1969.
[18] Q. H. F. Vrehen, A. Broese van Groenou, and J. G. M. de Lau, "Anisotropy broadening of ferromagnetic resonance in dense Ni–Co ferrites," *J. Appl. Phys.*, vol. 40, p. 1426, Mar. 1969.
[19] M. Weiner and S. Dixon, Jr., "Subsidiary resonance in planar hexagonal ferrites," *IEEE Trans Magn.*, vol. MAG-6, pp. 397–399, June 1970.

An Improved Equivalent Circuit for the Thin-Film Lumped-Element Circulator

REINHARD H. KNERR, MEMBER, IEEE

***Abstract*—A program written for the Hewlett-Packard automatic network analyzer permits the *S*-parameter eigenvalue phases and magnitudes to be displayed. The thus measured eigenvalues of a lumped-element circulator lead to an improved equivalent circuit which explains the observed "double hump" characteristic. The influence of different circuit parameters on the eigenvalues is measured and found in good agreement with the author's previously published theory. It is concluded from this theory and the measurements that, for the lossy circulator in general, maximum isolation, return loss, and minimum forward loss do not occur at the same frequency.**

I. Introduction

IN A PREVIOUS PAPER [1] the author developed a theory on the thin-film lumped-element circulator using the eigenvalue analysis [2]. The computer results which were obtained from this theory improved our understanding of circulators in general and were applied to a new broad-banding principle [1], as well as to a new switching principle for circulators [3].

The availability of a computerized network analyzer has since made it practical to measure eigenvalue phases and magnitudes as a function of frequency using the proper computer program. These measurements have permitted the principal results of the theory to be verified and have revealed additional information that has led to an improved equivalent circuit for the thin-film lumped-element circulator. Furthermore, the study has advanced our understanding of the losses in the lumped-element circulator and has permitted us to draw conclusions as to the behavior of lossy circulators in general.

Manuscript received September 15, 1972; revised January 21, 1972.
The author is with Bell Telephone Laboratories, Inc., Allentown, Pa. 18103.

II. Comparison of the Experimental Lumped-Element Circulator with the Calculation for the Earlier Equivalent Circuit

The broad-band thin-film lumped-element circulator (described in a previous paper by the author [1]) is shown schematically in Fig. 1. It uses the crossover capacitances as the sole means of resonating the circulator junction. Broad-band behavior is achieved with a capacitor formed by the dielectric layer between the metal film and ground plane of Fig. 1. This capacitor is designated C_0 in Fig. 2, which shows the approximate equivalent circuit of the structure in Fig. 1. The crossover capacitances are represented by the discrete capacitors C_1, while the split conductors of Fig. 1 are delineated by the inductors L, which are functions of the angular frequency ω, the geometry factor [1] G, the saturation magnetization, and the applied magnetic biasing field H_{dc}.

From this structure and its analysis [1] it was deduced that the capacitor C_0 influences only the eigenvalue of the in-phase excitation, and the capacitors C_1, i.e., the crossover capacitances, influence only the eigenvalues due to the rotating excitations or eigenvectors. (For details on eigenvalues and eigenvectors see the